Cave stratigraphy in western Norway; multiple Weichselian glaciations and interstadial vertebrate fauna

EILIV LARSEN, STEINAR GULLIKSEN, STEIN-ERIK LAURITZEN, ROLF LIE, REIDAR LØVLIE AND JAN MANGERUD

BOREAS

Larsen, Eiliv, Gulliksen, Steinar, Lauritzen, Stein-Erik, Lie, Rolf, Løvlie, Reidar & Mangerud, Jan 1987 09 01: Cave stratigraphy in western Norway; multiple Weichselian glaciations and interstadial vertebrate fauna. *Boreas*, Vol. 16, pp. 267–292. Oslo. ISSN 0300-9483.

Skjonghelleren is a marine-cut cave with 15–20 m thick pre-Holocene sediments. Corings and excavations reveal three beds of extremely fine-grained, laminated sediments alternating with blocky sediments. The laminated beds are interpreted as glaciolacustrine sediments deposited subglacially at times when ice sheets covered the area, suggesting at least three glaciations after the cave was formed. The blocky/diamictic sediments were formed by frost-shattered blocks from the roof of the cave during ice-free periods, and mixing with the fines through slow mass movements along the floor of the cave. In the diamictic sediment beneath the uppermost laminated bed, almost 7,000 bone and teeth fragments of birds, mammals and fish were found. Birds dominated, with little auk and brunnich's guillemot as the most frequently occurring species. Arctic fox was the dominating mammal. During climatic optimum of the interstadial, conditions seem to have been similar to present-day coastal Finnmark, with North Atlantic warm water entering the Norwegian Sea. Two radiocarbon dates on bones and three Uranium series dates on speleothems from this bed all cluster around 30,000 B.P., i.e., the end of the Ålesund interstadial. Above the uppermost laminated bed, bone fragments of birds, fish and mammals, deposited between *c.* 12,000 and *c.* 10,000 B.P., were found. Little auk dominate. The occurrence of squirrel is worth noting since it is limited mainly to areas with coniferous forest today. The beds below the 30,000 B.P. bed are poorly dated or undated, but it is tentatively concluded that the entire sediment sequence was deposited during the Weichselian stage. It seems that the cave was formed at a high relative sea-level stand sometime during the Early Weichselian. Two recorded palaeomagnetic excursions seem to correlate with the Laschamp/Olby and the Lake Mungo events, respectively.

Eiliv Larsen, Geological Survey of Norway, P.O. Box 3006, N-7001 Trondheim, Norway; Steinar Gulliksen, Radiological Dating Laboratory, NAVF, Norwegian Institute of Technology, N-7034 Trondheim-NTH, Norway; Stein-Erik Lauritzen, Department of Chemistry, University of Oslo, P.O. Box 1033, Blindern, N-0316 Oslo 3, Norway; Rolf Lie, Zoological Museum, University of Bergen, Muséplass 3, N-5000 Bergen, Norway; Reidar Løvlie, Geophysical Institute, Section C, University of Bergen, Allégt. 70, N-5000 Bergen, Norway; Jan Mangerud, Geological Institute, Section B, University of Bergen, Allégt. 41, N-5000 Bergen, Norway; *31st October, 1986 (revised 11th February, 1987).*

Skjonghelleren is a wave-cut cave positioned well above the post-glacial marine limit. Like many other caves in western Norway (Holtedahl 1984) it therefore must pre-date the last glaciation here. Reusch (1877a, b) and Undås (1942) described a thick sequence of laminated clay and silt in the cave, which they interpreted to have been deposited in a lake, dammed marginal to or beneath the ice during the last glaciation. The interpretation has been widely accepted, and is indeed the one we still favour. Undås (1942) also found a bone of a bird (puffin) below the laminated sediments, suggesting the possibilities of fossil-bearing strata of interstadial or interglacial age.

The corings proved a sediment depth of about 20 m, as already suggested by Reusch (1913), and we found three sequences of laminated clay, suggesting that the cave has survived at least three glaciations since its formation. Four blocky units were formed in ice-free periods prior to, between, and after the deposition of the laminated sequences. Bones were found in the upper, post-glacial, blocky unit, and thousands more bones were found in the next upper bed, dated by radiocarbon and U/Th to around 30,000 B.P. The age is also supported by palaeomagnetic results.

Coastal caves in Norway were investigated at an early stage (e.g. Reusch 1877a, 1877 b, 1913;

Kaldhol 1930; Undås 1942), but nearly forgotten by geologists, except for the studies by Holtedahl (1984). Our investigation demonstrates that these caves may hold extremely valuable information on on the Late Quaternary history of the area.

The cave

Skjonghelleren is developed into the steep slope forming the inner limit of the strandflat (Larsen & Holtedahl 1985) on the western side of the island of Valderøya (Fig. 1). The highest mountain on Valderøya is 231 m above sea level. The fjord between the islands Valderøya, Giske and Vigra has a maximum depth of 76 m. The bedrock on Valderøya consists of coarse crystalline, granodioritic gneisses; in nearby areas calcite-bearing gneisses and inclusions of limestone have been described (Gjelsvik 1951). Calcite is also found in the gneiss at Skjonghelleren (Table 1). The cave itself is formed along a fracture striking 275°–095° with a northerly dip between 50° and 60° (Fig. 2). The deepest part of the cave (or maximum sediment thickness) is therefore assumed to be below the northern wall. The seismic profile (Fig. 3) indicates that the level of bedrock is 30 m above sea level at the opening (beyond the limit of Fig. 3), increasing to nearly 45 m above sea level within the cave. With the cave floor at 63 m above sea level, this gives a sediment thickness of *c.* 20 m.

The cave is about 100 m long; its inner 70 m are shown in Fig. 3. The great sediment thickness indicates that the cave continues beyond this position. The height of the cave varies between 1 and 10 m, the width between 2 and 12 m. From 0 to 25 m (as measured from the inner limit) the cave is very narrow (Fig. 3) as a result of sediment-fill; the bedrock cave, however, has a relatively constant width.

All heights refer to mean sea level (Fig. 3). Chronostratigraphic nomenclature follows Mangerud *et al.* (1974) except that the Middle/Late Weichselian boundary is moved to 25,000 B.P. (Mangerud & Berglund 1978).

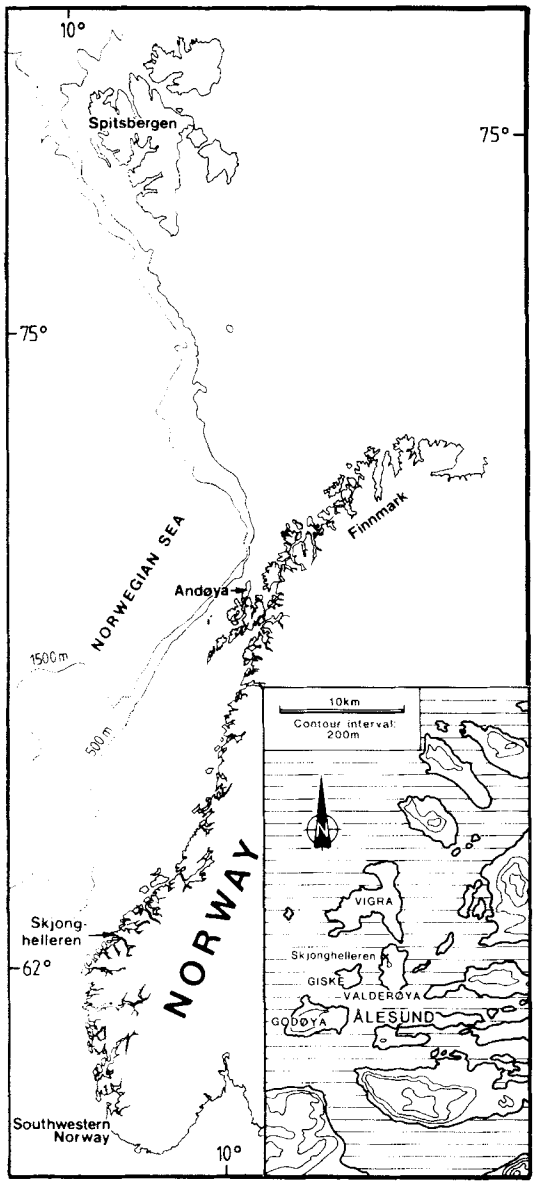

Fig. 1. Key map of Norway with names used in the text. A map of the Ålesund area with the cave Skjonghelleren (cross mark) on the island of Valderøya is inserted. Horizontal hatching is the sea.

Excavations and corings

The manually excavated sites, with letter designations of the walls, are shown in Fig. 3. The corings were made by a mobile wire-line drilling unit utilizing both hammer and rotation principles using 1 m long sampling tubes (inner diameter between 51 and 56 mm). The corings were made at three different angles from the base of excavation 1 in order to reach the deepest part of the cave at that site.

Fig. 2. View of the cave, developed along steeply dipping joints in the bedrock (gneiss). The opening is up to *c.* 30 m high. Photo towards east.

Excavation 1 and corings 1, 2 and 3

The first excavation was near the opening, and nearly 5 m deep (Figs. 3 and 5). From earlier descriptions (Reusch 1877a, 1877b; Undås 1942; Vibe-Müller 1963) and a small accessible section, we knew that a relatively thick sequence of laminated sediments existed at the site (Fig. 4). Undås (1942) reported a bone of puffin probably found in the bed we have labelled diamicton with bones G (Fig. 5). The corings extended from the base of excavation 1 down to bedrock. Coring was continued for 3.8 m into bedrock in order to be confident that it was not a block. The sedimentological descriptions of the corings are preliminary, but additional information is unlikely to influence the stratigraphic interpretations.

Excavation 2

This 6 m deep excavation (Fig. 6) is near the inner end of the cave (Figs. 3 and 7). The excavation uncovered the most complete stratigraphy and the least post-depositional disturbances.

Excavation 3

Excavation 3 was a narrow trench made to facilitate lithostratigraphic correlation between excavations 1 and 2 (Figs. 3 and 8). Within laminated clay F, individual lamina could be traced along most of the trench (Fig. 8), and also identified in excavations 1 and 2. Thus the sediments in the two main excavations can be correlated in great detail (Larsen et al. 1984). The correlations demonstrate that excavations 1 and 2 penetrated to the same stratigraphic level.

Lithostratigraphy and sedimentology

All lithostratigraphical units were defined in the field. The beds were given informal lithological designations. Letters were used for each bed described in the field (Figs. 5 and 6); the same letter corresponds to the same bed in each excavation.

Three groups of facies are recognized (Figs. 5 and 6): the facies associated with the fine-grained

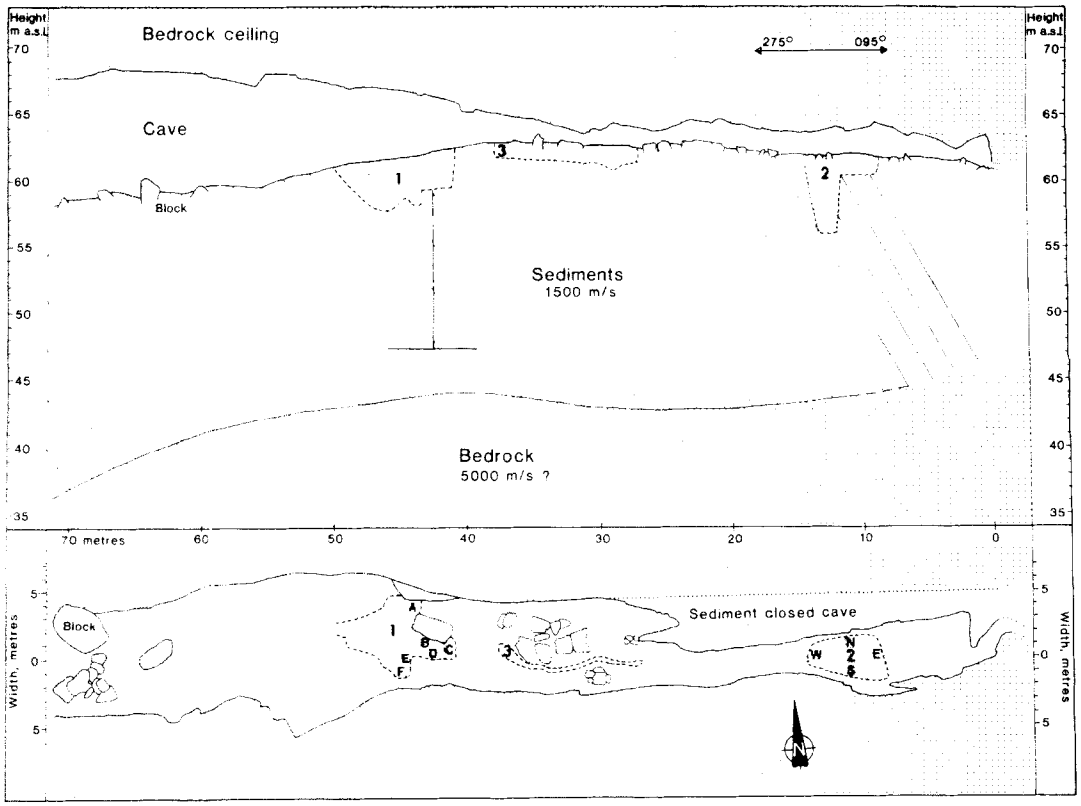

Fig. 3. Longitudinal profile (top) and map (bottom) of Skjonghelleren. The excavations are marked 1, 2 and 3. The deepest coring from the base of excavation 1 is shown. The section walls are marked A to F in excavation 1 and N, E, S and W (north, etc.) in excavation 2. S. Indrelid surveyed the cave. The sediment thickness is according to refraction seismics performed and interpreted by G. Hillestad.

sediments, those associated with the blocky sediments, and the speleothems. The alternations (cyclic) between the fine-grained and blocky sediments are interpreted to represent glacial vs. interstadial episodes.

The damming of water

The extremely fine-grained character of laminated clay L, I and F (Figs. 5 and 6) clearly proves deposition in quiet water; the complete lack of microfossils indicates a non-marine environment. Two alternatives for water in the cave can be seen: damming by sediments or by glacier ice. A sandur below two tills on the islands of Godøya and Vigra (Fig. 1) is described by Landvik & Mangerud (1985), and palaeocurrent reconstructions clearly indicate that the sandur also extended to the lower parts of Valderøya. This sandur could have dammed the cave, causing deposition of clay in a backwater pond. However, we find it highly improbable that this situation should be repeated three times (Beds L, I, F, Figs. 5 and 6). Also, the complete lack of sand in such thick fine-grained sequences is difficult to understand in a sandur environment.

An ice dam (Reusch 1913; Undås 1942) seems to be the only possibility to explain the laminated sediments. The area has been glaciated a number of times during the Weichselian (Mangerud 1981, 1983; Sejrup in press), so this is a reasonable repetitive mechanism.

Facies descriptions and interpretations

Laminated clay facies. – This facies completely dominates beds L, I and F (Figs. 5 and 6); it is not found in other beds. It is characterized by the fine grain size and the fining upwards laminations (couplets). Normally, the lamina thickness varies between *c.* 1 mm and *c.* 2 cm, and is on average greatest in excavation 1, where a maximum thick-

Fig. 4. The cave in the area of excavation 1. The left wall of the excavation is shown in Fig. 5, as are the cores extending downwards from the base of the excavation. The fence is about 1 m high.

ness of 5 cm occurs. The sediments also tend to be coarser in excavation 1 than in excavation 2. The contact between couplets is normally sharp. The laminated sediments are draped on the underlying sediments (Fig. 9). This, in addition to post-depositional compaction, control lamina dips. The compaction increases towards the north due to increasing sediment thickness. Small-scale faults accompany this general northerly dip. In excavation 2, average dip below bed G is higher than above, as one would expect (Fig. 6). The upper boundary of the laminated facies sequence is always erosional.

We have previously concluded that the laminated sediments were deposited in an ice-dammed lake. The high clay content, the long continuous laminations and the lack of frost-shattered material from the roof (see below), indicate that the cave was totally water-filled. The topographic position of the cave makes it difficult to envisage a lateral lake with a water level high enough to completely fill the cave. We thus conclude that the sediments were deposited subglacially. The lack of till and glaciotectonic disturbances show, however, that the glacier did not squeeze into the cave. Probably the water in the cave had a hydrostatic pressure proportional to the thickness of ice. By accepting the total ice-cover model, still to be explained are the sediment provenance, the cause of the rhythmicity and the sediment dispersal and sedimentation mechanisms.

As expected, the grain size difference between the two excavations (Figs. 5 and 6) shows an inward transport component. An X-ray diffractogram from laminated clay F in excavation 1 (Fig. 10) shows very little or no evidence of montmorillonite or other 14 Å minerals, which would be expected if the clay originated from the fracture above the cave (Carrol 1970). A SEM analysis of quartz grains from the same bed (Fig. 11) shows typically glacially-sculptured surfaces (Krinsley & Doornkamp 1973; Whalley & Krinsley 1974; Strass 1978). We conclude that the sediments are glacially derived, and transported into the cave in water.

The rhythmic nature is not fully understood. It must be related to discharge and sediment load variations, but whether these variations are caused by climatic changes (annual?) or simply reflect subglacial channel migrations or channel overflows (Röthlisberger 1972) is unclear.

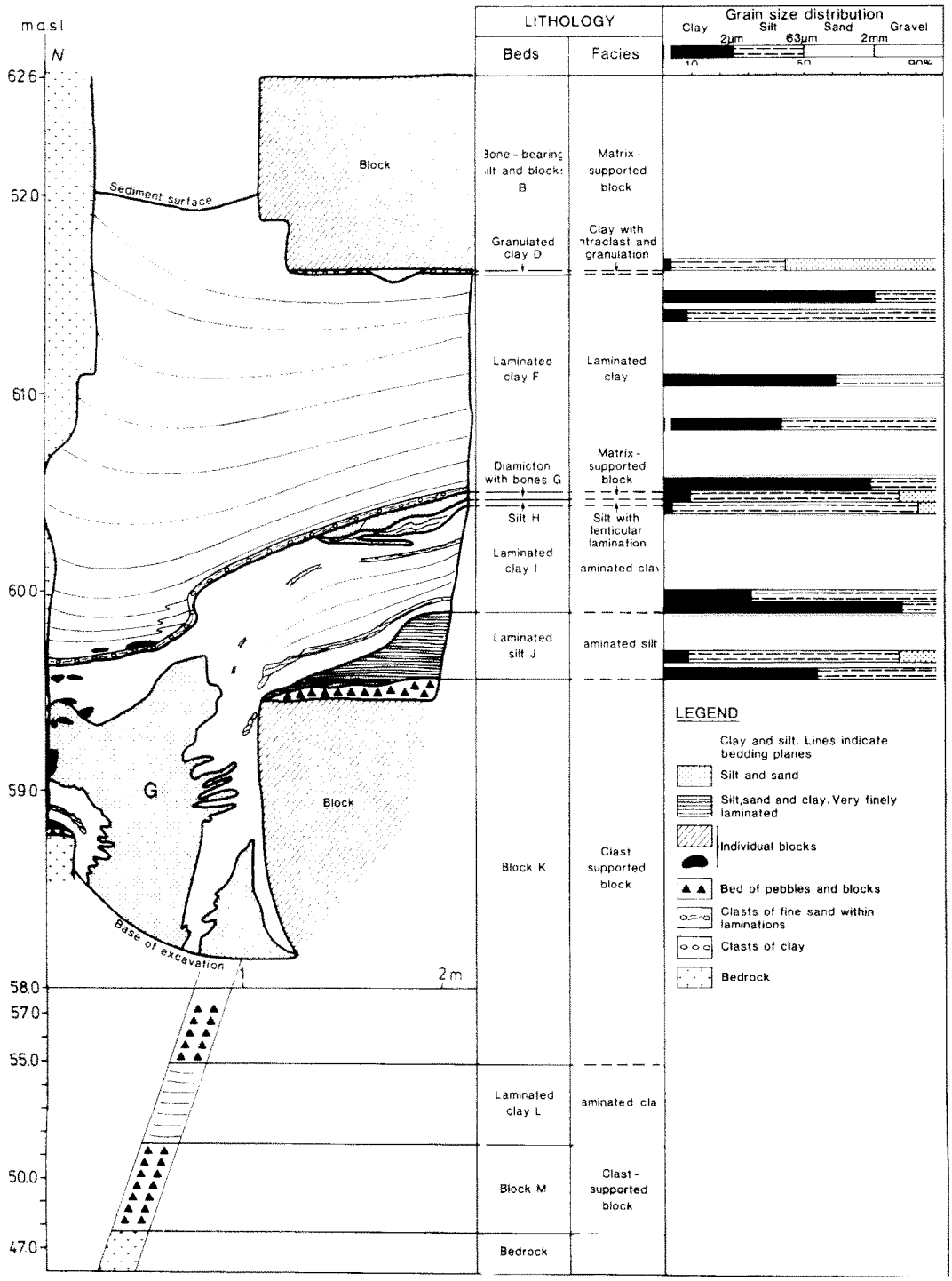

Fig. 5. Stratigraphy of wall A, excavation 1, plus the deepest coring extending from the base of the excavation. Grain-size analyses of material less than 16 mm are shown. The coring was at an oblique angle. Note change in scale between excavated and cored parts.

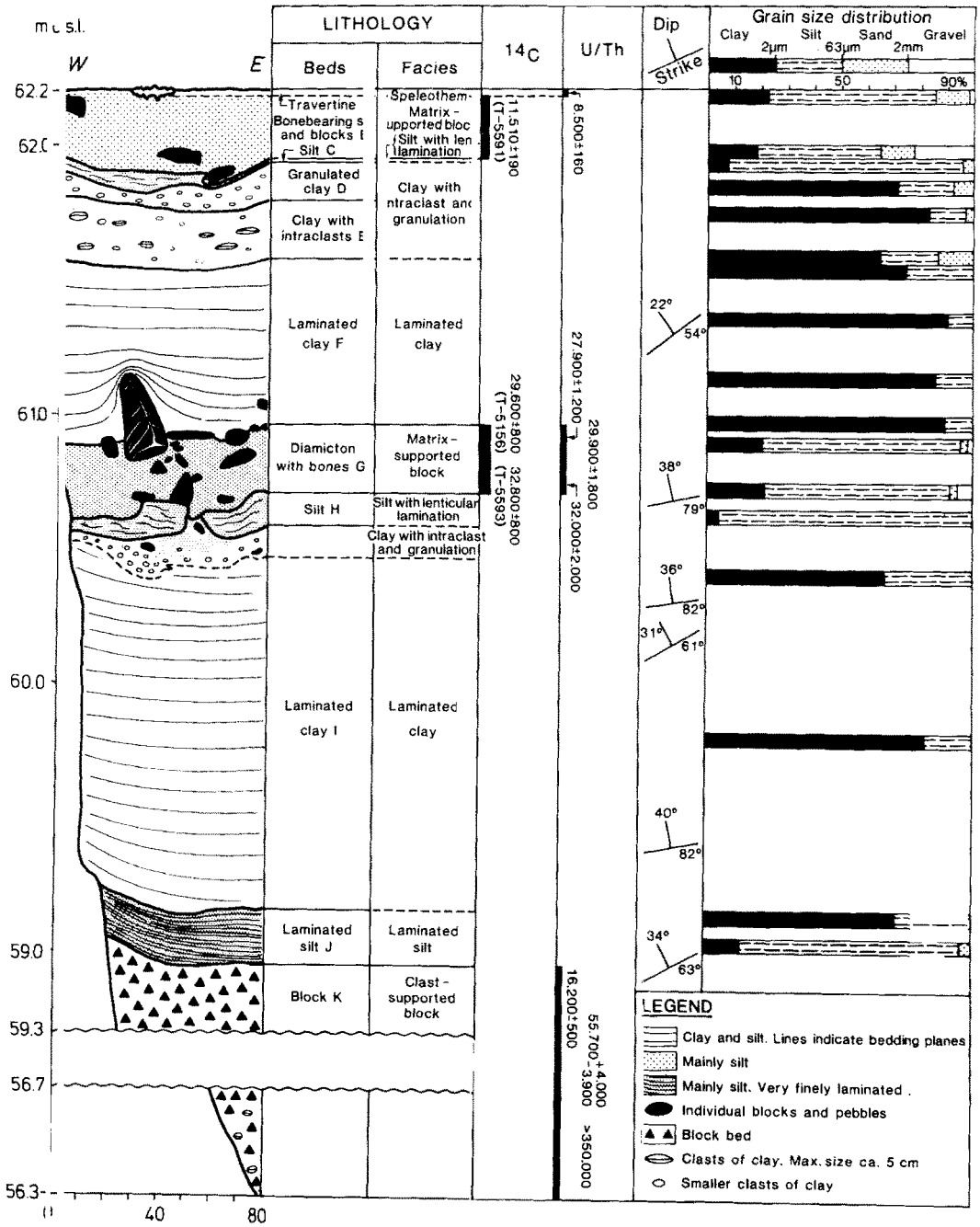

Fig. 6. Stratigraphy of the central part of the northern wall, excavation 2. Datings, bed orientations and grain-size distributions are included.

Fig. 7. The cave in the area of excavation 2. The excavated site is in the foreground, the cave opening in the background. Photo looking west.

Some deductions can be made, however, about transportation of material within the cave and about the sedimentation process. An inwards transport component is well documented by grain size differences. Because of post-depositional deformation it is difficult to compare the depositional levels between the sites, but laminated clay F was deposited in shallower water in excavation 2 further into the cave than in excavation 1. This implies that sediment transport occurred in the water column rather than as density currents. The draping (Fig. 9) supports the interpretation of deposition from suspension. The inferred transportation mechanisms suggests a very slow, laminar inward flow of the entire water column. A crude estimate of the maximum flow rate can thus be obtained by considering settling velocities. During deposition of bed I, the height to the cave ceiling at excavation 2 was about 4 m. Most particles greater than 2 μm were deposited farther into the cave. It takes about 24 days for 2 μm particles to settle 4 m in still 0°C water. If we suppose that the ice dam was 70 m farther away (Fig. 3), a 2 μm particle could spend a maximum of 24 days over these 70 m. This reflects a horizontal flow rate of a maximum of 3 m per day. This model suggests that the water drained through the cave, probably through fractures in the bedrock.

Laminated silt facies. – Some silt laminae exist in other beds, but the facies dominates only laminated silt J (Figs. 5 and 6). The bed is draped over block K. At the base there are a few clay–silt couplets with a gradational transition to mm-thin couplets composed mainly of silt, but with some fine sand (Fig. 5). A couple of clay–silt couplets are found *c.* 2 cm below the upper boundary. These are followed by a few silt to fine-sand laminae just below bed I. The laminae fine upwards. Normally the upper boundary is gradational, except for an unconformity in parts of excavation 1 caused by local slumping. The overall bed is thinner in the inner excavation (Figs. 5 and 6).

The gradual transition to laminated clay I suggests that this silt also was deposited in the ice-dammed lake. The greater contrast between laminae probably reflects greater discharge variations. The coarser fraction reflects higher flow velocities, compared to the laminated clay facies. The bed was probably deposited at a higher altitude at the

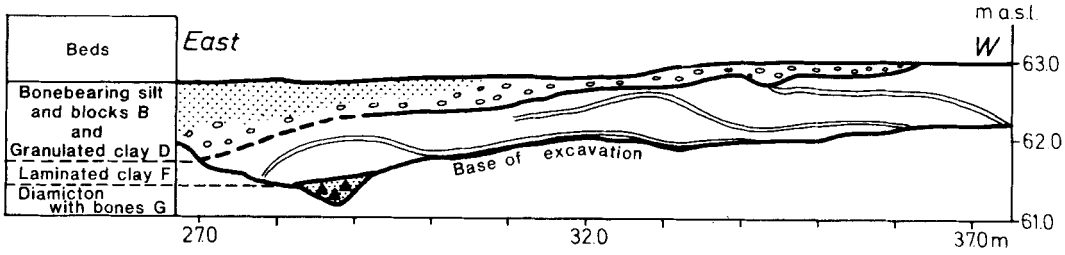

Fig. 8. Stratigraphy of the southern wall of excavation 3. The main laminae, recognized in laminated clay F in excavations 1 and 2, are indicated with parallel lines. ^{14}C dated bones, from the transition zone between beds D and B, gave an age of 10,360 ± 170 B.P.

position of excavation 1 (Figs. 5 and 6); it thins and fines inwards. It is therefore probable that at least the coarsest sizes were transported and deposited by density currents. The occurrence of clay couplets indicates periods of quiet water, and that the cave might have been totally water-filled. The observations suggest that this facies was deposited during the initial phases of the lake with glacier margin in the vicinity of the cave, causing a more variable sediment supply and generally higher energy environments than father back into the ice.

Laminated clay F is not underlain by a laminated silt facies. In excavation 1, however, the base of the bed has a 3 cm thick zone of laminated clay containing subangular clasts of fine sand (Figs. 5 and 12). This indicates a relatively high energy level during the initial phase of the lake.

Clay with intraclast and granulation facies. – The laminated clay facies is followed by the intraclast and granulation facies (Figs. 5 and 6). The facies has a lower erosional boundary and is best developed above laminated clay F in excavation 2, where the E and D beds are distinguished (Fig. 9). The facies is, however, also clear in the top of bed I (Fig. 6). The lower erosional boundary and the clasts were probably formed by water that drained out of the cave during deglaciation, causing erosion and redeposition of the clay in the cave.

Silt with lenticular lamination facies. – This facies is represented by bed H in excavations 1 and 2 and bed C in excavation 2 (Figs. 5 and 6). It is characterized by diffuse, lenticular and non-persistent laminations (Fig. 13). In excavation 1, the lower boundary was erosional, but the facies lies condordantly upon the underlying beds in excavation 2.

The sediment is presumed to have been deposited by sheet floods during the final draining of the cave during deglaciation.

Clast-supported block facies. – The term 'block' is used for large (>256 mm), angular rock fragments showing little or no modification by transporting agents, with a surface resulting from breaking of the parent mass (Bates & Jackson 1980). An angularity distinguishes blocks from boulders. Units K and M are composed of numerous blocks, but hereafter are called block K and block M. Block K by definition is entirely of this facies, probably also most of bed M, and pockets in bed G.

Parts of block K were excavated at both sites 1 and 2, but the bed is penetrated only by the cores. Large clasts of laminated clay near the base of excavation 2 indicate that it nearly penetrated to laminated clay L. With the exception of the lower and upper parts of the bed, practically no matrix exists between the blocks, but a thin veneer of clay is common on the block surfaces. Block K is composed mainly of angular blocks and stones. The largest block encountered (cored) was about 2.4 m across. In the excavated part of site 1, block K is composed of one large block covered by an up to 38 cm thick layer of gravel and stones (Fig. 12). All blocks and stones are the local gneiss, except for the clasts of speleothems and vein calcites in excavation 2. The concentration of these clasts is greatest near the base of the bed, but they do occur throughout the bed, between the other fragments.

Block M is almost 4 m thick and is recorded only in cores (Fig. 5). The largest block was some 85 cm across. Voids existed between the blocks, but due to cooling water being used in the coring process, little is known about the matrix between blocks. One of the cored fragments showed some degree of rounding. All blocks have been derived from the local bedrock.

This facies is interpreted to be blocks weathered from the roof. Most blocks apparently fell during cold periods with active frost weathering. Few blocks were found above the Holocene cultural remains, suggesting that thick block beds represent

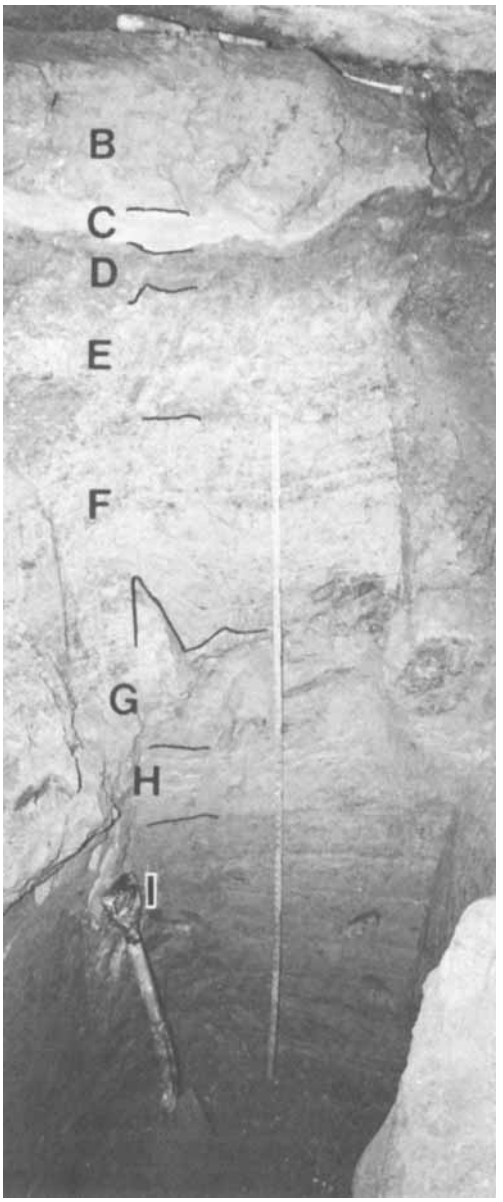

Fig. 9. Northern wall, excavation 2, showing beds I–B. Beds K and J are in the shadow.

long, cool periods. Due to the observation of one rounded boulder in block M and the stratigraphic position of this bed, it may have been exposed to marine action. In fact, it may be assumed that wave-abraded boulders grade upwards to frost-shattered blocks as a consequence of regression during an interstadial.

Matrix-supported block facies. – This facies consists of blocks similar in appearance and origin to the clast-supported block facies. The difference is that the blocks are supported by a fine-grained matrix. However, there are all transitions, from the openwork blocks without any matrix, to a silt with few floating blocks.

This facies dominates beds B and G, where the overwhelming number of bones were found. A stratigraphic description is therefore useful.

In bed G in the inner excavation (Fig. 6), the matrix is dominated by clay and silt, and the sediment can best be described as a diamicton. In the middle to upper part of the bed, voids are common between the blocks. Well defined clasts of clay and silt are common. At this site, more than 6,000 bone fragments and several fragments of speleothems and vein calcites were found. There are higher concentrations of bones in the lower, mainly silty part of the bed. The amount of bones decreases upwards, and there were none in the uppermost part. Speleothem fragments were found only in the lower and middle parts of the bed, but not as deep as the deepest bone fragments. A few very small fragments of charcoal were found in bed G in excavation 2. Two of these samples (el 83043 and -091) are supposed to be *Pinus* and *Alnus* (L. M. Paulsen pers. comm. 1983). The first was actually found in laminated clay F, but was probably redeposited from bed G.

In excavation 1, bed G can be subdivided into a lower and an upper unit separated by an erosional boundary. The lower part is composed mainly of silt with fine sand and subangular clasts of clay. In the upper part, clay dominates. Stones, blocks and bone fragments are less frequent in excavation 1 than in excavation 2. Speleothems and vein calcites are not found in excavation 1.

In both excavations, the lower boundary of the facies is erosional.

The bone-bearing silt and blocks B in excavation 2 is dominated by silt, in which there are some floating clasts of clay, blocks, stones and bones. The sediment is mainly massive, but with some diffuse, subhorizontal bands. Small folds exist along the boundary towards silt C. The bed is found only in a depression in the northern part of the excavation, and wedges out towards the east, west and south. Most bones were found in the upper part, but bones were scattered throughout the bed.

In excavation 1, bed B is a silt and sand pocket where one bone fragment was found.

In pit 2 (Fig. 6), all beds have a strike parallel to

the long axis of the cave (E–W), and a northerly dip which is greater below bed G than above it (Fig. 6). The lower boundary of bed G is erosional and the bed thickens towards the north. These observations are best explained by originally horizontal beds being deformed towards greatest sediment thickness (north), and a simultaneous slow mass movement (solifluction) in the same direction. An incomplete vertical mixing of bed G, however, is indicated by a fauna development through the bed and the lack of bones and speleothems in the uppermost part.

Bed B is folded, either by sliding or solifluction. The fold axis is almost parallel to the long axis of the cave. Farther towards the north (outside the fold), bed B wedges out.

The matrix in the block facies derives from the underlying and overlying fine-grained sediments. This is best seen from the inclusion of clasts of laminated clay in the matrix. Underlying clay was incorporated by solifluction or simply by squeezing when blocks fell from the roof. We assume that the bulk of the matrix was incorporated by solifluction, but some was also incorporated during deposition of the overlying clay bed.

Speleothem facies. – This facies consists of speleothems, mainly carbonates, precipitated on the cave floor.

Only bed A (Fig. 6), and other post-glacial precipitates on floor, ceiling and walls, are *in situ*. However, this facies has also been repeated, as fragments are found as clasts in beds G and K. These clasts are formed by frost shattering. Bed A displays classic speleothem shapes (stalactites, stalagmites and botryoidal forms). All remaining samples consist of tabular, frost-shattered clasts, lacking stalactitic shapes, but may well have formed as crusts on the surfaces in the cave.

In addition to the speleothem clasts, beds G and K also contain clasts of vein calcite originally formed in the cavity above the cave. For chronological purposes it is essential to distinguish between the two groups of carbonates, because speleothems formed during ice-free periods within the cave whereas vein calcite pre-dates the cave.

Speleothem deposition in non-carbonate caves is rare, but is previously reported from Norway (Schrøder 1984). The speleothems have a distinct internal structure (laminations, growth bands) distinguishing them from coarse crystalline vein fragments. They are either pure calcium carbonates (travertime A, Table 1, Fig. 6) or they contain mixtures of laumontite, rhodochrosite, K-feldspar and quartz in addition to calcium carbonate (samples el 83020, -112, -307A, -044, -142 and -221, Table 1). K-feldspar and quartz obviously are impurities, whereas laumontite and rhodochrosite are probably formed as secondary precipitates along with the calcium carbonate. Laumontite and rhodochrosite have not been previously reported from speleothems (Hill 1976; White 1976). However, large, pink stalagmites and stalactite consisting of rhodochrosite do exist in one Bulgarian cave (Dr. K. Spassov pers. comm. 1986).

The origin of the constituents in the speleothems may be discussed in detail. $CaCO_3$ is found both in the cavity (el 83107, Table 1) and in the gneiss itself (el 83108 and -137, Table 1). The main $CaCO_3$ source is probably vein calcite. Both rhodochrosite

Table 1. Results of X-ray diffractometry on bedrock and speleothem samples.

Sample	Bed/Site	Type of material	Minerals
el 83108	Bedrock, mountain above cave	Gneiss	Quartz, Feldspar (Plagioclase, K-feldspar), Mica, Calcite
el 83137	Bed G	Clast of gneiss	Quartz, Feldspar (Plagioclase, K-feldspar), Chlorite, Calcite
el 83107	Cavity above cave	Vein mineral	Calcite
el 83020	Bed K	Speleothem clast	Calcite, Laumontite
el 83112	Bed K	Speleothem clast	Calcite, Laumontite
el 83307A	Bed K	Speleothem clast	Calcite, Laumontite
el 83307B	Bed K	Clast of vein mineral	Calcite
el 83044	Bed G	Speleothem clast	Calcite, Laumontite
el 83142	Bed G	Speleothem clast	Calcite, Laumontite, Rhodochrosite?
el 83221	Bed G	Speleothem clast	Calcite, Rhodochrosite, Laumontite, Anorthite, Quartz
el 83023	Bed A	*In situ* speleothem	Calcite

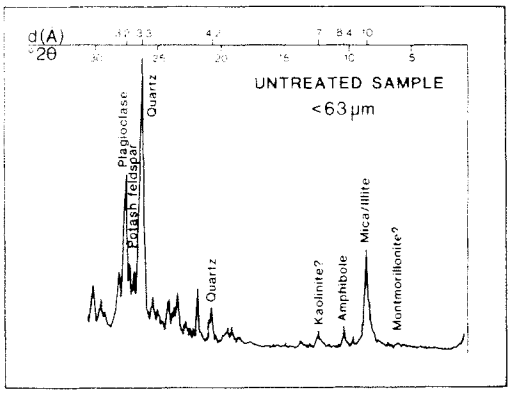

Fig. 10. X-ray diffractogram from laminated clay F, excavation 1 (sample el 83002).

Fig. 11. Scanning electron microscope photo of quartz grain from laminated clay F, excavation 1 (sample el 83001). Grain shows conchoidal fractures and steps. Bar scale = 100 µm.

and laumontite are found in veins and as secondary precipitates (Berry & Mason 1959). The precipitates may be an alteration product from plagioclase and glass (Berry & Mason 1959). Sample el 83307B (Table 1) from bed K is a coarse crystalline vein calcite.

Local palaeoenvironment

According to our interpretations, the sediment sequence reveals three periods of total ice cover (the fine-grained sediments) and, including the post-glacial, four ice-free periods (the blocky sediments). The fining up from J to I and the lower part of F (Fig. 6) may indicate that sedimentation of the fine-grained sediments took place at least partly under advancing glaciers. Palaeomagnetic data support the interpretation of rapid sedimentation for bed F shortly after deposition of bed G. In the upper part of the laminated sequences, erosional and redepositional structures are attributed to draining of the cave when the damming glacier thinned. The magnitude of these erosional events is unknown, but is inferred to be small. The observations suggest that the later phases of the glaciations were non-depositional.

Both solifluction and frost shattering (the blocky sediments) generally reflect a cold climate with repeated freeze–thaw cycles. The abundance of blocks in these beds, compared with the Holocene surface, the correlations (Fig. 16) and datings, indicate that the blocky sediments were formed in cool, but ice-free periods during the Weichselian. The formation of speleothems (beds K, G and B) reveals the existence of groundwater circulation. This means that at least for parts of these periods there was no permafrost. Both frost shattering and speleothem formation rule out the possibility that beds M and K were deposited in an open cave under a cold-based glacier simply because both processes require water. Travertine A is found undisturbed overlying bed B (Fig. 6). It therefore seems that mass movements had ended when bed A was deposited some 8,500 years ago.

Dating

Absolute dates were obtained in excavations 2 (Fig. 6) and 3. The results are listed in Tables 3 and 4.

Radiocarbon

Identified bones (Table 2) were selected for radiocarbon dating. All dates but one (T-5593) were performed on bones from several species.

Collagen was separated from the bones by the following method: After initial washing and crushing to fragments <2 mm, the bone material was hydrolyzed with 3 N HCl at room temperature under reduced pressure. Insoluble residue was treated at 5% NaOH (room temperature) for 5 min and collagen dissolved in water at 90°C, adjusted to pH 3.0–3.5 with HCl. This ensured that

Table 2. List of species dated by radiocarbon (Table 3). Species names are given in Tables 5 and 6.

^{14}C laboratory reference number	Dated species	
T-5156	*Alopex lagopus*	Phocidae
	Plautus alle	Alcidae
	Uria lomvia	Unidentified mammalia
	Calidris maritima	Unidentified aves
	Fratercula arctica	Unidentified pisces
	Cepphus grylle	
	Pollachius virens	
T-5591	*Alopex lagopus*	Anatidae
	Pusa hispida	Unidentified mammalia
	Plautus alle	Unidentified aves
	Cepphus grylle	Unidentified pisces
	Melanitta fusca	
	Lagopus mutus	
	Somateria mollissima	
	S. spectabilis	
T-5592	*Plautus alle*	*Uria* sp.
	Cepphus grylle	Phocidae
	Fratercula arctica	Unidentified mammalia
	Somateria spectabilis	Unidentified aves
	Larus marinus	Unidentified pisces
	Anarhicas lupus	
T-5593	*Uria lomvia*	

contaminating humic acids not removed by the alkali treatment were precipitated. Insoluble remains were removed by centrifugation before evaporation to recover the gelatine. This was combusted to CO_2 and counted in gas-proportional counters. The collagen separation technique eliminates contamination efficiently. With this collagen extraction technique, a mammoth tusk from Fåvang, earlier dated at 20,000 B.P. (T-1239), was dated at >47,000 B.P. (T-2801, S. Gulliksen, unpubl.).

Sample gas was analysed for ^{13}C, and activity measurements normalized to $\delta^{13}C = -25‰$ rel. PDB. No correction for reservoir age was applied.

The yield of carbon (Table 3) gives only a rough estimate of the collagen preservation status, as the extraction procedure is not designed for accurate determination of the content. The figures, however, are quite consistent with the mean values obtained for regular bone samples dated in the laboratory (3.6 ± 1.9%).

Although radon contamination should not be a serious problem for gelatin samples, this possibility was investigated by measuring T-5156 after normal storage time of 3 weeks and again after 16 weeks. No significant difference was observed between measurements.

At this site the possibility of introducing modern carbon is small, as the samples were collected more than 70 m from the opening of the cave, where no plant cover exists. Modern carbon might be transported in ground water through the cavity above the cave, and introduced from cultural beds on top of the excavation. The dated bed, however, is sealed by the overlying very impermeable laminated clay F (Fig. 6), which effectively limits water penetration. The amount of water dripping from fractures in the cave ceiling is very little, and the

Table 3. Radiocarbon dates on bone samples.

Laboratory reference number	Sample reference	Age B.P. $\pm 1\sigma$	$\delta^{13}C$ 0/00 rel. PDB	Yield %gC/g Bone
T-5591	Bed B excavation 2	11,510 ± 190	−16.0	1.3
T-5592	Bed B excavation 3	10,360 ± 170	−17.2	3.5
T-5156	Bed G excavation 2	29,600 ± 800	−16.3	1.4
T-5593	Bed G excavation 2	32,800 ± 800	−15.6	2.4

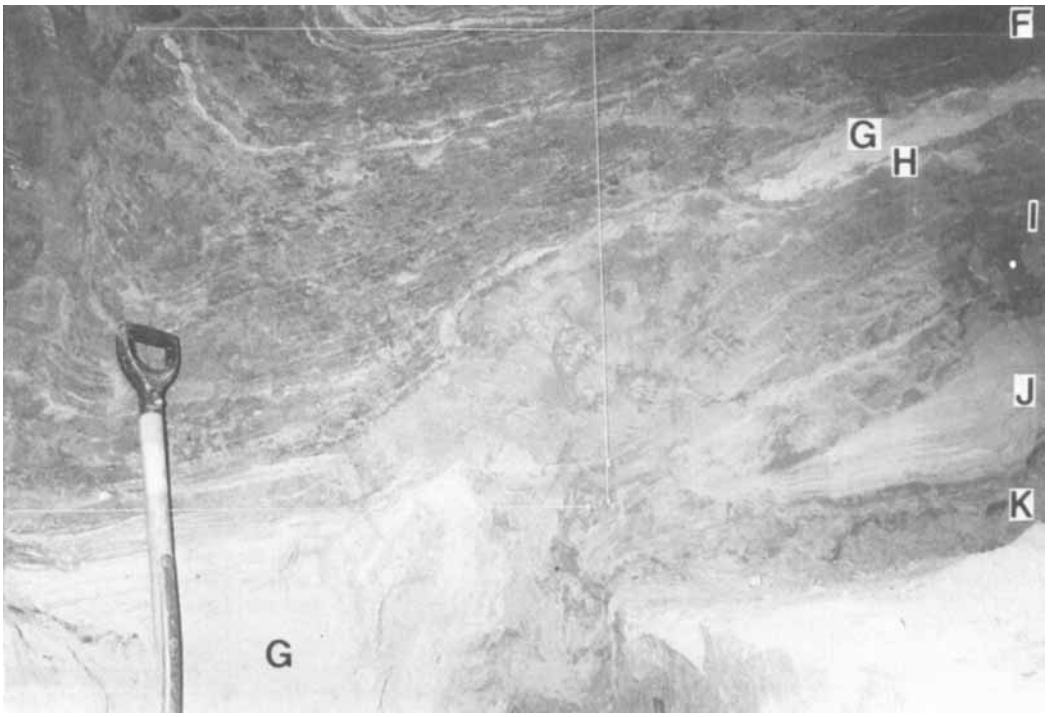

Fig. 12. Section wall A, excavation 1. In the lower left corner diamicton with bones G has slumped into laminated clay I. The same bed (G) is in the upper right corner. Above the two parts of G, at the base of laminated clay F, laminations with silt/sand clasts can be traced continuously. These laminations form the basis of a small basin in the lower left.

Fig. 13. Diamicton with bones G between silt H (lower left corner) and laminated clay F. In the centre a *c.* 5 cm long bone of ringed seal. Several of the white spots are speleothem fragments. From the northern wall, excavation 2.

ground-water table is far below the dated bed. In addition, it is difficult to imagine how any introduced modern carbon could form chemical compounds sufficiently identical to collagen, or having sufficiently strong chemical bonds to it, to withstand removal during the extraction process. We thus conclude that contamination is a minor problem and that the age difference between the dates from bed G (Fig. 6) is real and caused by random selection of bones from a layer spanning some thousand years.

Uranium series

Seven speleothem dates were obtained from excavation 2, one of them a flowstone crust (bed A) on top of the sediment sequence, three on fragments from bed G, and three on fragments from block K. In addition, one test was performed with uranium series dating on bones from bed G (el 83159), and one sample of vein calcite (el 83307 B) was dated. The samples were dated by the $^{230}Th/^{234}U$ disequilibrium method. The mineralogy of the dated samples is presented in Table 1.

Speleothems in non-carbonate caves are often exceptionally rich in uranium due to the high uranium content of the surrounding bedrock. Most of the present samples have a high uranium content (Table 4), considering that the material contains *c.* 30% insoluble silicates (all samples except el 83023 and -159). The samples are therefore considered well-suited for dating.

The dated samples were selected on the basis of their internal structure (e.g. they were laminated, secondary deposits), distinguishing them from vein fragments. Sample el 83023 is a 5–10 mm thick botryoidal crust, taken *in situ* on top of bed B (Fig. 6). The remaining samples were angular clasts from beds G and K (Fig. 6). Sample el 83044 showed secondary solution pitting (1–2 mm diameter), whereas the other two had intact surfaces. All three samples showed a similar internal lamination of white and pink bands.

The samples (2–7 g) were cleaned in dilute acid prior to analysis. They were then digested in HNO_3; the gelatinous residue from laumontite was then treated with $HF/HClO_4$ until dissolution was complete. All leachates were combined before further processing of each sample. U-concentration, activity ratios of $^{234}U/^{238}U$, $^{230}Th/^{232}Th$ and $^{230}Th/^{234}U$, were determined by the isotope dilution technique, chemical separation of U and Th fractions, and radiometric determination by alpha particle spectrometry. A $^{228}Th/^{232}U$ spike was used as the internal standard. This spike was calibrated against a standard uraninite in 1981 and 1983, and its activity ratio was calculated before each batch of samples. Furthermore, interlaboratory calibrations reveal a good accuracy relative to other U-series laboratories. The spectra were corrected for background and decay after separation of the spike mother and daughter nucleides. The age was calculated from the activity ratios of Table 4. The error is based only on the counting statistics.

Table 4. Uranium Series Disequilibrium dates of speleothems, vein calcite and bones. The $^{230}Th/^{234}U$ ratio of el 83112 is corrected for ^{228}Th tailing in the spectra. Maximum tailing gives 23.5 ka, which is the youngest possible age. 80.1 ka is the best estimate. Sample el 83307B shows evidence of post-depositional leaching of uranium.

Sample	Bed	Material	U conc. ppm	$^{234}U/^{238}U$	$^{230}Th/^{232}Th$	$^{230}Th/^{234}U$	Age B.P. $\pm 1\sigma$
el 83023	A	*In situ* speleothem	39.2	1.30	>1,000	0.075	8,500 ± 160
el 83044	G	Speleothem clast	4.09	1.38	>1,000	0.244	29,900 ± 1,800
el 83142	G	Speleothem clast	1.50	1.46	28.7	0.229	27,900 ± 1,200
el 83221	G	Speleothem clast	1.84	1.55	>1,000	0.259	32,000 ± 2,000
el 83159	G	Bones of *Pusa hispida*	621.7	1.42	>1,000	0.104	11,800 ± 1,200
el 83020	K	Speleothem clast	5.61	1.36	8.2	0.140	16,200 ± 500
el 83112	K	Speleothem clast	3.35	1.42	>1,000	0.538 −0.197	$80{,}100\ ^{+\ 8{,}700}_{-\ 8{,}200}$ −23,500 ± 3,300
el 83307A	K	Speleothem clast	0.985	1.50	26.2	0.412	$55{,}700\ ^{+\ 4{,}000}_{-\ 3{,}900}$
el 83307B	K	Clast of vein material	0.976	1.35	11.1	1.682	>350,000

The samples contain far more uranium than the lower detection limit of the method (>0.05 ppm). Acceptable to high chemical yields (17–58%) of U and Th ensured sufficient activity for counting. However, experiments with increasing counting times and tail correction of the ^{228}Th and ^{230}Th peaks suggest that a 2σ error should be used in correlation of the dates. Except for two samples, ^{230}Th/^{232}Th ratios are high (>20), indicating that contamination from detrital thorium is negligible. ^{234}U/^{238}U ratios are fairly similar for all samples (mean ratio 1.42 ± 0.08) and typical for terrestrial environments (Szabo & Rosholt 1982) and other Norwegian speleothems. There is therefore no detectable evidence of post-depositional migration of uranium (except for vein calcite sample el 83307B). The samples appear dense and crystalline, satisfying the conditions for the requirement of a closed system since deposition.

In situ speleothems are younger than the surface they rest upon. Hence, sample el 83023 post-dates bed B. However, speleothem clasts have grown elsewhere and have fragmented some time after they were precipitated. In general, they are therefore of equal or greater age than the surface they rest upon and older than the sediment which buries them. Because the diamicton with bones G experienced mass movements, we can say only that the speleothems are of the same age or older than the enclosing sediment.

The speleothem dates of this study support the widely-held assumption that speleothems grow preferentially under non-glacial conditions (Lauritzen & Gascoyne 1980, and references cited therein, Lauritzen 1984).

Like mollusks, bones do not contain much uranium *in vivo*, the phosphate and organic matrix of bone acts as an effective scavenger for uranium in the percolating ground water of the burial site. After some time (x), an 'equilibrium' in the uranium uptake may be assumed. Hence, a uranium series date (t) always represents a minimum age, where the 'true' age is $t + x$ years. (x) may vary from a few ka to about 15 ka (Szabo 1980; Schwarcz 1982). Uranium series dating of bone should therefore work better for older than for younger material.

Bones of ringed seal (30 g, sample el 83159) from bed G were crushed, cleaned of internal clay by flotation and washing, and dated using a modified extration procedure. The uranium yield was acceptable (13.7%), whereas the thorium yield was very low (1.2%) (Table 4). In order to compare this date with the radiocarbon dates of bones from the same bed (Fig. 6), the necessary value of (x) must be high (18–20 ka). Further discussion is dependent on results from more samples.

Of the four samples from the porous bed K, two may be rejected (el 83020 and el 83307B) because of probable ^{232}Th contamination and/or evidence of uranium leaching (^{230}Th/^{234}U > 1.0). Of the remaining two samples, el 83307A is considered analytically correct, while sample el 83112 resulted in a spectrum with considerable tailing of the ^{228}Th peak. Tail correction yielded a best estimate of 80 ka, whereas the youngest possible age ('worst estimate') is 23.5 ka.

Palaeomagnetic properties

General results

The results of detailed palaeo-rockmagnetic and magnetic fabric analysis of 124 oriented samples from beds J, I, H and F, pit 2, reported elsewhere (Løvlie & Sandnes 1987), can be summarized as follows: the depositionally-related remanent magnetization in beds J, I and F (carried by magnetite grains <2 μm has probably not been modified by post-depositional distortions or compaction during consolidation. Palaeomagnetic directions thus reflect genuine records of the geomagnetic field. Partially demagnetized (thermal/alternating field), single component directions describe high-amplitude variations of inclination (sub-horizontal to 80°), represented by declinations distributed between east – south – west (Fig. 14). These anomalous palaeomagnetic directions, which are not in accord with a normal configuration of the Late Quaternary geomagnetic field, are interpreted to record two geomagnetic excursions.

Bed H carries steeply-dipping palaeomagnetic directions compatible with the present geomagnetic field. The origin of magnetization in this bed, however, is not necessarily related to the actual deposition, as falling blocks, constituting bed G, may have induced a shock remanent magnetization parallel to the ambient geomagnetic field (Symons *et al.* 1980). Bed H was probably deposited during the draining of the cave, preceding accumulation of the blocky bed G. The palaeomagnetic directions in bed H thus record the geomagnetic field preceding or coinciding with the onset of the Ålesund interstadial some 33 ka ago (Fig. 16). Similar considerations also apply to the origin of the steeply-dipping palaeomagnetic inclinations

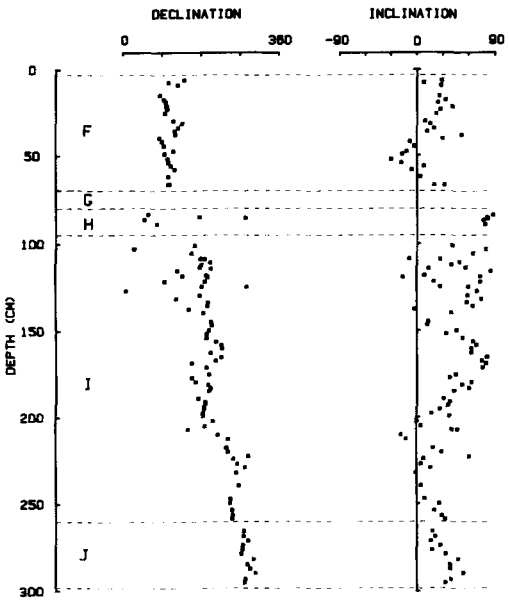

Fig. 14. Stratigraphic plot of univectorial palaeomagnetic directions in excavation 2 after partial alternating field demagnetization to 40 mT. Lithologic units, bold letters to the left, are indicated by broken lines.

in the laminated clay bed L, overlain by the blocky bed K.

Geomagnetic excursions

Virtual geomagnetic poles (VGP), based on five-points running mean directions (univectorial), define very consistent paths, as shown on the Mercator projection in Fig. 15. During formation of beds J and I (<56 ka), the VGP display two meridionally constrained paths situated around 90°W and at the site longitude. This characteristic of some transitional field geometries (Hoffman 1982), suggesting that the excursion may present an aborted geomagnetic reversal. The predominantly non-dipole configuration of the geomagnetic field during reversals implies that synchronous VGPs from different regions may not necessarily coincide. Hence, on a global scale an instability of the geomagnetic field is likely to be reflected by different VGP signatures. From these considerations, the excursion in beds J and I is correlated with the Laschamp/Olby event, dated by different methods to have occurred between 36 and 42 ka (Gillot *et al.* 1979). Within this time interval, additional regional records of inferred excursion have been encountered in Denmark (Rubjerg low-inclination excursion, Abrahamsen & Knudsen 1979) and in Arctic Ocean sediment cores (Løvlie *et al.* 1986).

The three counterclockwise VGP loops (Fig. 15) are interpreted to represent the behaviour of the non-dipole field during an aborted reversal. Assuming a life-span of *c.* 1,000 years for a complete non-dipole cycle (Denham 1974), estimates for the duration of this high-resolution record

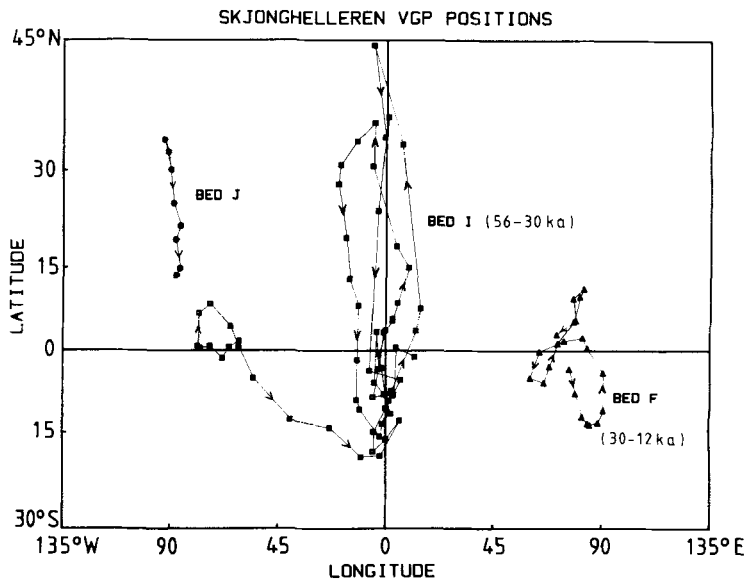

Fig. 15. Mercator projection of virtual geomagnetic pole positions for beds J, I and F, based on 5 points running mean (univectorial).

range from 500 to 3,000 years, depending on whether the paths are interpreted to represent 1, 2 or 3 complete secular variation cycles, respectively.

None of the beds records a complete geomagnetic excursion VGP path, but attention is put to the steeply-dipping inclinations residing in the beds deposited prior to (bed L) and after (bed H) deposition of beds J and I.

The gap in the VGP path between top bed J and base bed I evidences a short depositional hiatus between the two beds.

Bed F (<29 ka) defines two equatorial, counterclockwise VGP loops between 60° and 90°E and 15°S and 10°N. Considering that this VGP path probably represents a high-resolution, incomplete record of geomagnetic excursion, the correlation with one synchronous VGP determination (spot-reading) for the Lake Mungo excursion (fire-place F12, 28,000 ± 410 B.P., 47°E, 6°S, Barbetti & McElhinny 1976) is remarkably good. The oldest Lake Mungo event spans some 2,000 years (30 to 28 ka), and is represented by three spot-readings of equatorial VGPs covering 180° of longitude (Barbetti & McElhinny 1976). The two small amplitude VGP loops recorded in bed F are thus likely to represent a time span considerably less than 2,000 years.

Vertebrate fauna

Remains from vertebrate faunas older than 20,000 years are extremely rare in Norway (Mangerud 1981). Here, we have identified more than twenty species from beds dated around 30,000 B.P. (Table 5).

Identification and description

The overwhelming percentage of the bones were found in bed G (Table 5), and most of them in excavation 2. The few bones in bed F are assumed to have been redeposited from G, and the bones ascribed to bed H could, in the field, be genetically related to bed G. Nearly 7,000 bones (Table 5) were collected from this level, being around 30,000 years old. Another group of approximately 1,000 bones (Table 6) were collected from bed B, being 10,000–12,000 years old.

No whole skeletons were found. However, some bones belonging to the same animal, and parts of jaws with several teeth were recovered. Bone sizes varied between a few mm and some 6 to 7 cm.

The samples were carefully washed on a 1 mm sieve and dried at room temperature. Clay particles attached to bones were removed by careful brushing or scraping. Most bones were well preserved and well suited for identification. Identifications were carried out either with the naked eye or occasionally at 2–4× magnification; always comparing with a modern reference collection. The level to which bones can be determined is mainly dependent on bone preservation and whether they contain diagnostic features. The more difficult bone fragments were identified by three persons working independently. This was the case for example when trying to distinguish between brunnich's guillemot and atlantic murre.

During most of the sampling the individual bone-bearing beds were sampled as one unit. But during the later period of the field work, bed G in excavation 2 was divided into a lower (L), a middle (M) and an upper (U) zone. Due to lack of stratification, the boundaries between the three zones are arbitrary and may have varied somewhat between persons during the sampling period.

The vast amount of bones from bed G are from birds, mostly little auk and brunnich's guillemot. Arctic fox is the dominating mammal.

Six hundred and ninety-four fragments were collected from the transition zone between beds D and B in excavation 3, and are all included in bed B (Table 6). Birds dominate and little auk is the most common species.

From the identified species, it appears that species diversity was lower during deposition of bed B than during bed G (Tables 5 and 6). Some species not identified in the latter, however, are found in B: Mountain hare, squirrel, velvet scoter, eider duck, greater black-headed gull and four-bearded rockling.

Palaeoecology

Ålesund interstadial (Figs. 5 and 6). – According to our interpretations, the bones in beds F, G and H (Table 6) belong to the same ice-free period centred around 30,000 B.P., the Ålesund interstadial (Fig. 6). From this level, about 17 times as many bones were found in excavation 2 as in excavation 1 (Table 5). The investigated volume of sediments from this bed was roughly comparable in the two excavations, but only a small volume was investigated in excavation 3. We assume that differences

Table 5. List of species in or derived from bed G (Figs. 5 and 6) in all three excavations. During field work, bed G in excavation 2 was sampled from a lower (L), middle (M) and upper (U) zone. R is the remaining which was not sampled with regard to internal subdivision of the bed. T gives the total sum of each species within diamicton with bones G in excavation 2.

	Excavation 1		Excavation 2						Excav. 3
	Bed G	Bed F	Bed G					Bed H	Bed G
Latin (English. Norwegian) names			L	M	U	R	T		
MAMMALIA (Mammals. Pattedyr).									
Pusa hispida (Ringed seal. Ringsel).			2			3	5		
Alopex lagopus (Arctic fox. Fjellrev).			8			35	43		
Lutra lutra (Fish otter. Oter).			1				1		
Lemmus lemmus (Norway lemming. Lemen).	1					1	1		
Phocidae (True seals. Seler).			2				2		
Canidae (Canids. Hunder).			1				1		
Unidentified	49		15			100	115	1	
Total	50		29			139	168	1	
AVES (Birds. Fugler).									
Plautus alle (Little auk. Alkekonge).	45		123	69	1	351	544		
Uria aalge (Atlantic murre. Lomvi).			1	1			2		
Uria lomvia (Brunnich's guillemot. Polarlomvi).			156	28	1	85	270		
Fratercula arctica (Puffin. Lunde).			12	3		1	16		
Cepphus grylle (Black guillemot. Teist).			8	1		2	11		
Somateria spectabilis (Spectacled eider. Praktærfugl).				1			1		
Larus canus (Mew gull. Fiskermåke).				1			1		
Rissa tridactyla (Kittiwake. Krykkje).			2				2		
Pagophila eburnea (Ivory gull. Ismåke).			1				1		
Stercorarius parasiticus (Arctic skua. Tyvjo).			1				1		
Calidris martima (Purple sandpiper. Fjæreplytt).			1			1	2		
Fulmarus glacialis (Fulmar. Havhest).				1			1		
Lagopus mutus (Rock ptarmigan. Fjellrype).						2	2		
Uria sp. (Murres. Lomvier).			38			17	55		
Alcidae (Auks. Alker).			131	17	1	18	167		
Anatidae (Ducks and geese. Ender).				1		3	4		
Unidentified	283		2,172	626	15	2,189	5,002	18	1
Total	328		2,646	749	18	2,669	6,082	18	1
PISCES (Fishes. Fisker).									
Gadus morhua (Atlantic cod. Torsk).			3				3		
Pollachius virens (Pollock. Sei).						1	1		
Brosme brosme (Cusk. Brosme).			2				2		
Myoxocephalus scorpius (Shorthorn sculpin. Vanlig ulke).			1				1		
Anarhicas lupus (Atlantic wolffish. Gråsteinbit).		1							
Unidentified		3	27			163	190		
Total		4	33			164	197		
UNIDENTIFIED			61				61		
TOTAL SUM	378	4	2,769	749	18	2,972	6,508	19	1

Table 6. List of species from bed B in excavations 2 and 3.

Latin (English. Norwegian) names	Bed B	
	Excav. 2	Excav. 3
MAMMALIA (Mammals. Pattedyr).		
Pusa hispida (Ringed seal. Ringsel).	2	
Alopex lagopus (Arctic fox. Fjellrev).	1	
Lepus timidus (Mountain hare. Hare).	1	
Sciurus vulgaris (Squirrel. Ekorn).		4
Phocidae (True seals. Seler).		2
Canidae (Canids. Hunder).		1
Rodentia (Rodents. Gnagere).		2
Unidentified	5	7
Total	9	16
AVES (Birds. Fugler).		
Plautus alle (Little auk. Alkekonge).	26	110
Fratercula arctica (Puffin. Lunde).		3
Cepphus grylle (Black guillemot. Teist).	5	2
Melanitta fusca (Velvet scoter. Sjøorre).	1	
Somateria mollissima (Eider duck. Ærfugl).	4	
Somateria spectabilis (Spectacled eider. Praktærfugl).	1	3
Larus marinus (Greater black-headed gull. Svartbak).	1	1
Lagopus mutus (Rock ptarmigan. Fjellrype).	2	
Uria sp. (Murres. Lomvier).		1
Anatidae (Ducks and geese. Ender).	1	
Unidentified	303	550
Total	344	670
PISCES (Fishes. Fisker).		
Enchelyopus cimbrius (Four-bearded rockling. Firtrådet tangbrosme).	1	
Anarhicas lupus (Atlantic wolffish. Gråsteinbit).	1	1
Unidentified	3	
Total	5	1
UNIDENTIFIED		7
TOTAL SUM	358	694

in depth of burial and sediment properties are too small to have caused significant variations in preservation conditions (Figs. 5 and 6). However, the preservation conditions might have been somewhat different before burial due to more exposure to light at the outermost site. We did not observe any difference in preservation and the percentage of identifiable bones is similar in the two excavations. The difference in number, therefore, is concluded to be due to larger primary deposition of bones at the site of excavation 2.

Only three species were identified from excavation 1, whereas twenty-one were identified to species level in excavation 2 (Table 5). The most common species in both excavations was little auk (11.3% of the total in excavation 1, 8.3% in excavation 2). In excavation 2, arctic fox and brunnich's guillemot are also numerous; all other species occur in small numbers. If all species are represented in the same relative abundance in the two excavations, the probabilities of finding 0, ≥ 1, ≥ 2 and ≥ 3 identifiable fragments of arctic fox in excavation 1 are respectively: 9.3%, 90.7%, 74.9% and 49.5%, within one standard deviation. Because no fragments of arctic fox were identified in this excavation, we suggest that the differences between the two sites are caused by primary deposition, i.e. the innermost site was preferred by scavengers and hunters (see below).

There appear to be two main alternative explanations for the accumulation of bones: First, the animals themselves may have sought the cave. Second, some or most of the animals may have been taken into the cave by other animals or by man. The first point to be made is that fish must have been taken in, since there are no indications of any direct marine influence on the sediments. It is also extremely unlikely that seals would have

found the long, dark cave attractive. As far as we know, birds have never been observed far into the cave today. We conclude that most, if not all, bones were taken into the cave. None of the identified species is able to catch seals, and when seals suffer a natural death, they almost exclusively do so at sea and sink to the bottom. Compared with the present-day Arctic, the easiest explanation would be that polar bears killed the seals, and that all or most of the bones were taken into the cave by the arctic fox, known to hoard during summer. The presence of charcoal in bed G in excavation 2 could be an argument for human impact, but the finds are few and fragments small, and they might have been blown into the cave during or after a natural fire in the area. During most of the excavation of bed G, Svein Indrelid, Archaeological Museum, University of Bergen, participated, but found no evidence of man.

The species belonging to the family Alcidae (little auk, brunnich's guillemot, puffin, black guillemot and Atlantic murre) all nest in colonies, suggesting that the cliff into which Skjonghelleren is developed was a nesting cliff. It is therefore likely that the fauna is mainly a summer fauna. Obvious exceptions are arctic fox, Norway lemming and rock ptarmigan, which do not migrate during the year. This demonstrates that food was present during the winter, too.

Today pollock and cusk are common along the Norwegian coast, but are normally not found north or east of Finnmark. The spawn in waters with temperatures between 6°C and 9°C, and avoid waters colder than 4–5°C. The presence of fish otter indicates that open water existed in or close to the area also during the winter. These observations support the conclusion by Mangerud *et al.* (1981a), based on the presence of *Arctica islandica*, that Atlantic water reached the coast of western Norway during the Ålesund interstadial. This conclusion is also compatible with indications of a relatively warm interval in oxygen isotope stage 3 in cores from the Norwegian Sea (Streeter *et al.* 1982), but not with the reconstructions by Kellogg (1977) and Kellogg *et al.* (1978).

Ivory gull, found in the lower part of bed G, together with e.g., cusk and otter, suggests a different environment, as it lives only in the area of sea-ice cover. Today, ivory gull visit Finnmark only occasionally during the winter. Two interpretations of this apparent conflict are possible, the simplest being that the faunas are of slightly different ages, because there was obviously a deglaciation, ice-free, glacial readvance cycle during the Ålesund interstadial (Mangerud *et al.* 1981a). The other possibility is that the summer/winter contrast was larger than in coastal Finnmark today.

Norway lemming and rock ptarmigan demonstrate that vegetation existed. Two of the charcoal fragments were identified as *Pinus* and *Alnus*. If correct, and if these trees grew in the area, rather favourable conditions must have prevailed. Little is known about vegetation in this period, but Mangerud *et al.* (1981a) identified pollen in Ålesund interstadial samples. In addition to *Pinus*, the most frequently occurring pollen grains were *Betula*, *Juniperus*, *Artemisia*, Poaceae, Cyperaceae and other unidentified herb pollen grains. Mangerud *et al.* (1981a) concluded that an open vegetation with some birch existed at some interval during the Ålesund interstadial. Possibly, *Pinus* and *Alnus* were also present, implying a climate not colder than that of western Finnmark today. This conclusion is compatible with the warmth-demanding vertebrate fauna discussed above. However, the presence of *Pinus* and *Alnus* is questionable.

Some significant differences exist between the lower and the middle parts of bed G in excavation 2 (Table 5). Brunnich's guillemot is most common in the lower part but little auk strongly dominates the middle part. The present distribution of these species overlaps, but little auk is the most high-arctic. Together with the fish remains, this indicates a warmer climate during deposition of the lower part of bed G than during the middle part (Table 5). If we postulate that ivory gull represents the earliest immigration after deglaciation, the fauna in the lower part of bed G indicates a climate comparable to the coastal areas of Finnmark today. The lower species diversity, along with dominance of little auk in the middle part of bed G, indicates climatic conditions similar to western Spitsbergen today. We thus believe to have documented the cooling towards the next glacial advance over the site. Very few bone fragments were found in the upper part of bed G (Table 5), and the amount of frost-shattered blocks and stones increased, indicating a further cooling.

Bed B (Figs. 6 and 8). – Bone and teeth fragments from sediments deposited after the last deglaciation are listed in Table 6.

Species diversity is lower in bed B than in bed G. This may be due to the significantly lower number of bones which, in turn, may reflect the smaller

volume of sediments investigated. Little auk is the dominating species. An interesting difference between the two beds is the lack of brunnich's guillemot in bed B. This species is a more specialized fisheater than puffin and black guillemot, which are found in both formations. Little auk, also frequent within both formations, eats mainly plankton. Literally, this may indicate that a plankton supply was comparable in the two periods, while fish supply was sparser just after the last deglaciation. This interpretation is not straightforward, however, because a good plankton supply should favour the presence of plankton-eating fish. In addition, the data base for the interpretation is weak. The number of identified fish species is lower in bed B than in bed G (Tables 5 and 6), but the total number is too low to form the basis of a firm conclusion.

The presence of squirrel (Table 6) is surprising, as squirrel is found mainly in forests and prefers conifers. The nearest conifer prior to 10,000 was pine, which had its northern boundary in northwestern Germany and southern Sweden during the Allerød Chronozone (Berglund 1966). Mountain hare also has relatively low spreading potential, and for both these species the question of immigration route is problematic as the major part of Scandinavia was still ice-covered.

Conclusions: correlations and geological history

In this chapter we will start at the top of the stratigraphy, simply because the youngest history is best known.

Beds A and B

These beds were deposited after the last deglaciation. The date 11,510 ± 190 B.P. (Fig. 6) gives a minimum age for the last deglaciation in the Skjonghelleren area. Previous work (Mangerud *et al.* 1981a), however, demonstrates that the deglaciation occurred some time before 12.3 ka.

The two dates on bones from bed B gave Late Weichselian ages (Table 3). Apart from man-made ones (Vibe-Müller 1963), there are no known bone accumulations from the Holocene. During the Holocene the presence of man was apparently necessary for bone accumulations in the cave. During cooler periods (beds B and G) the mountain above the cave was a nesting cliff, and, in addition to man, arctic fox (or other animals) could take bones into the cave. At present we favour arctic fox as the 'transporting agent' for the bones.

Beds C, D, E and F

We have concluded that the laminated clay was deposited in a subglacial ice-dammed lake. Beds C–F are bracketed between radiometric dates of about 12.5 ka and 30 ka, and thus the damming glacier, at least in a general way, corresponds to the Weichselian maximum.

The palaeomagnetic correlations suggest an age of around 28 ka for bed F. This age is supported by the dates from bed G, and many shell-dates from the Ålesund interstadial (Mangerud *et al.* 1981a; Landvik & Mangerud 1985), of which the youngest are 28–30 ka. The obvious conclusion is that the ice front advanced into the area very close to 28 ka B.P.

The palaeomagnetic record also suggests that bed F was deposited in considerably less than 2,000 years. Thus, there is a hiatus in the sedimentological record of more than 10 ka (Fig. 16) between 28 and 12.5 ka. In all three excavations the sequence of beds F–E–D–C–B is found. The lower boundaries of E and B are erosional, so some sediments have been removed. Clearly, the erosional events between beds C and B are minor because the thin bed C is preserved. The erosion may have been larger between E and F, but we infer that this, too, was limited, as the same laminae are traced in the upper half of bed F in all three excavations. We conclude that there was a non-depositional hiatus between beds F and E in addition to the erosional hiatuses (Fig. 16). This can be explained easiest by assuming that the temperature regime under the ice changed after deposition of F, causing the lake-water to freeze. The conclusion is that there was a continuous ice cover from about 28 to 12.5 ka, as also suggested by Mangerud *et al.* (1981a).

From Skjonghelleren the continental edge is only about 65 km away, where the glacier would start to float. Thus the glacier front must have remained relatively close to its Weichselian maximum position for some 15 ka. This is very different from Andøya (Fig. 1), which has been essentially ice-free since 20 ka (Vorren 1978). The shelf edge is only 10–15 km outside Andøya, and the eastern and northern sides of the island are bounded by a deep and wide fjord. The Skjonghelleren area and

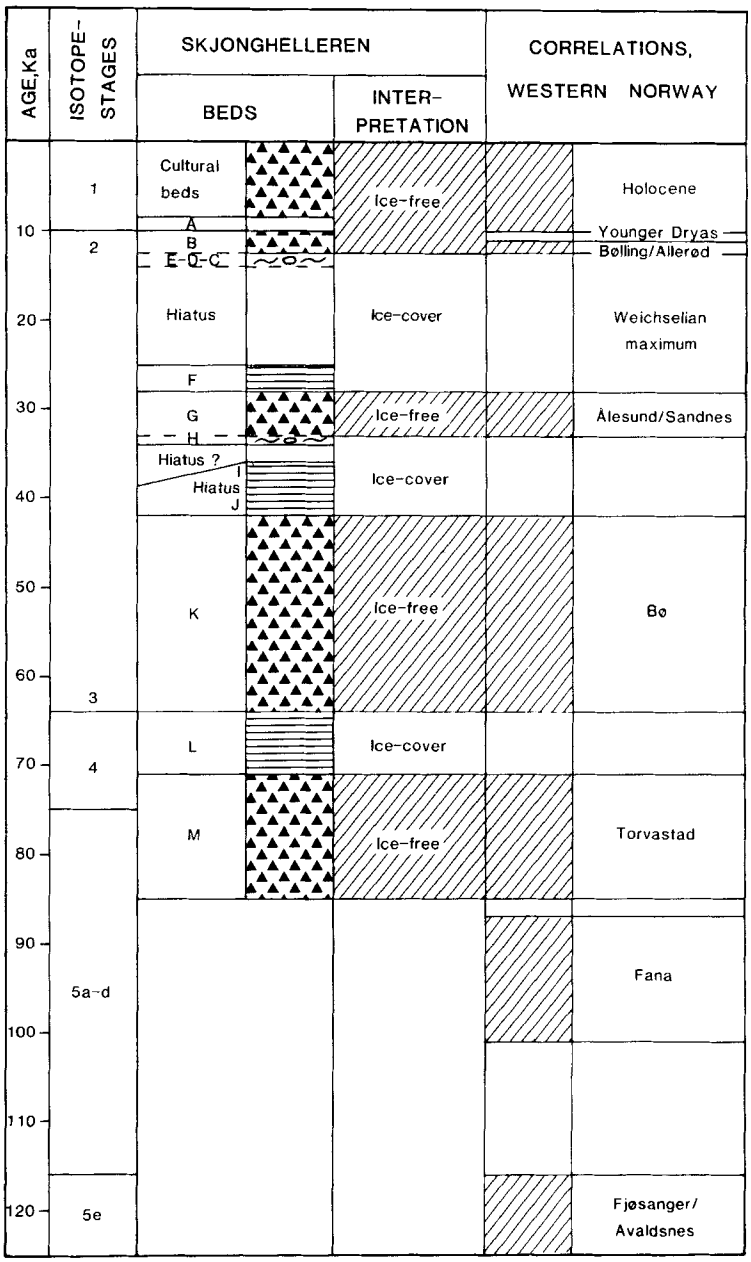

Fig. 16. Summary of the stratigraphy in Skjonghelleren compared to western Norwegian stratigraphy (according to Miller *et al.* 1983; Sejrup 1987). Erosional boundaries between beds in Skjonghelleren are shown with stippled lines. Inferred non-depositional hiatuses are also indicated.

Andøya are the two stretches along the coast with the narrowest continental shelf (Fig. 1). Whether the different glaciation histories are caused by regional differences in the ice-sheet behaviour, or simply by the fact that Andøya was located closer to the Weichselian maximum ice border, is unknown.

Bed G (Ålesund interstadial)

We have argued that both the radiocarbon and the U-series dates should be reliable; a conclusion stronly supported by the close agreement between all the dates. Thus the age of bed G is around 30 ka. One may also argue that the duration of the ice-

free period was short, because all dates range between 28 and 33 ka. We have, however, no stratigraphic control of the individual dates within the bed, and probably the cave was ice-free some time before the bones were taken in. Also there might have been a time lag before the formation of speleothems; the age of the dated post-glacial sample (8.5 ka) is 4,000 years younger than the deglaciation of the area.

When bed G is correlated to the stratigraphy outside the cave, it is clearly of Ålesund interstadial age (Mangerud *et al.* 1981a). Mangerud *et al.* concluded that the duration of the Ålesund interstadial was from 38 to 28 ka. However, some sites included in this interstadial are probably from older ice-free periods (Landvik & Mangerud 1985). At present bed G is the best 'type-locality' for the informal Ålesund interstadial s.s. If the obtained dates accurately represent the duration of the ice-free period, the Ålesund interstadial is a short event (some 5,000 years); if the duration was longer, the dates represent the younger part of the Ålesund interstadial.

Outside Sunnmøre the Ålesund interstadial is correlated with the Sandnes interstadial in southwestern Norway (Andersen *et al.* 1983) and also to an interstadial in northern Norway (Andreassen *et al.* 1984). Certainly, the climate inferred from the faunal remains in Skjonghelleren suggests that much of coastal Norway was ice-free during the Ålesund interstadial. This fauna also reinforces the earlier conclusion (Mangerud *et al.* 1981a) that a branch of the North Atlantic Current entered the Norwegian Sea, and reached at least as far north as Ålesund at this time.

Beds H, I and J

Palaeomagnetic correlations indicate that beds J and I were deposited in less than 2,000 years some time between 36 and 42 ka. The transition K–J is thus undated as is the lower limit of the Ålesund interstadial (Fig. 16). The VGP path from J to I (Fig. 15) indicates a brief hiatus, probably due to a period of non-deposition, as there is no visible erosion between the beds. Whether there is a non-depositional hiatus between I and H, as there is between F and E (Fig. 16), is not known, but it seems probable. Our data indicate that the ice advanced over the site some time between 42 and 36 ka before present and that this glacier event lasted between 500 and 9,000 years. The onset of this glaciation compares well with the inferred age of the end of the Bø interstadial (Miller *et al.* 1983; Sejrup 1987; Fig. 16).

Bed K

Bed K is poorly dated (Table 4). Analytical and geological arguments, however, are in favour of the date yielding 55 ka, the geological argument being the possible correlation to the Bø interstadial in southwestern Norway (Fig. 16). The thickness of bed K compared to beds B and G, indicates a long, cool period. This is compatible with the supposed duration of the Bø interstadial and its climate (Sejrup 1987; Fig. 16).

Bed L

The oldest recorded glacial advance over the area is undated.

Bed M and the formation of the cave

This bed, M, representing an ice-free period, is also undated. By counting from the top, a correlation with the Torvastad interstadial in southwestern Norway is possible (Fig. 16).

Any discussion of the age of the cave is speculative. Mangerud *et al.* (1979) suggested that the formation took place just prior to the last major Weichselian glaciation. A better guess now would be that the cave was formed during the ice-free period just before and during formation of bed M, possibly some 70 to 80 ka ago. Even if a neotectonic uplift has taken place in western Norway since the Eemian (Mangerud *et al.* 1981b; Holtedahl 1984; Sejrup 1987), a deglaciation phase with glacioisostatic depression is more likely to account for a relative sea level high enough to have formed the cave, as the bedrock floor of the cave (Fig. 3) is close to the Late Weichselian marine limit (Reite 1967; Greve 1984). This indicates a pre-bed M Weichselian glaciation, a contention in support of previously suggested composite stratigraphy for western Norway (Mangerud 1981, 1983; Sejrup 1987; Fig. 16).

Acknowledgements. – S. Befring, O. Longva, E. Danielsen, N. Meisfjord, S. Indrelid, P. Undheim, K. Sørgaard, G. Hillestad and J. Landvik participated during the field work. R. Sjøberg initiated the seismic investigation by arguing for great sediment thickness. L. M. Paulsen identified charcoal samples. T. Eldholm, A. Hansen, K.-J. Karlsen, K. Sand, Aa. Scheie, A. Storvik and S. Sæterbø provided technical assistance and performed laboratory analyses. M. Adachi, J. Ellingsen, L. Holiløkk and E. Irgens have drawn and reproduced illustrations. The

manuscript was typed by L. Øverby and J. G. Wesche. The English language was corrected by J. Reid who also read the manuscript critically. The Historical Museum, University of Bergen and the land-owner, B. K. Skjong, allowed investigations at this site protected by law. The work was financially supported by Elf Aquitaine Norge A.S., The Geological Survey of Norway (NGU), the University of Bergen, The Norwegian Research Council for science and the Humanities (NAVF) and Sunnmørsbanken A.S. To all these persons and institutions we proffer the most sincere thanks.

References

Abrahamsen, N. & Knudsen, K. L. 1979: Indication of a low-inclination excursion in supposed middle Weichselian interstadial marine clay at Rubjerg, Denmark. *Physics of the Earth and Planetary Interiors 18*, 238–246.

Andersen, B. G., Sejrup, H. P. Kirkhus, Ø. 1983: Eemian and Weichselian deposits at Bø on Karmøy, SW Norway: A preliminary report. *Norges geologiske undersøkelse 380*, 189–201.

Andreassen, K., Vorren, T. O. & Johansen, K. B. 1984: Pre Sen-Weichsel glasimarine sedimenter på Arnøy, Nord-Norge. *Abstract, 16. Nordic geological meeting*. University of Stockholm.

Barbetti, M. F. & McElhinny, M. W. 1976: The Lake Mungo geomagnetic excursion. *Philosophical Transactions of the Royal Society, London A 281*, 515–542.

Bates, R. L. & Jackson, J. A. (eds.) 1980: *Glossary of Geology*, 2nd ed. 751 pp. American Geological Institute. Falls Church, Virginia.

Berglund, B. E. 1966: Late-Quaternary vegetation in eastern Blekinge, south-eastern Sweden. I. Late-Glacial time. II. Post-Glacial time. *Opera Botanica 12*, 180–190.

Berry, L. G. & Mason, B. 1959: *Mineralogy. Concepts, Descriptions, Determinations*. 630 pp. W. H. Freeman and Company, San Francisco.

Carrol, D. 1970: Clay minerals: A guide to their X-ray identification. 80 pp. *Geological Society of America Special Papers*.

Denham, C. 1974: Counter-clockwise motion of palaeomagnetic directions 24,000 years ago at Mono Lake, California. *Journal of Geomagnetism and Geoelectricity 26*, 487–498.

Gillow, P. Y., Labeyrie, J., Laj, C., Valladas, G., Guérin, G., Poupeau, G. & Delibras, G. 1979: Age of the Laschamp palaeomagnetic excursion revisited. *Earth and Planetary Science Letters 42*, 444–450.

Gjelsvik, T. 1951: Oversikt over bergartene i Sunnmøre og tilgrensende deler av Nordfjord. *Norges geologiske undersøkelse 197*, 5–45.

Greve, S. 1984: Kvartære avsetninger på Vigra og Valderøya, Sunnmøre: Glasialkronologi, strandforskyvning og sedimentologi. 93 pp. Unpublished thesis, University of Bergen.

Hill, C. 1976: *Cave Minerals*. 150 pp. National Speleological Society, Huntsville, Alabama, USA.

Hoffman, K. A. 1982: The testing of geomagnetic reversal models: recent developments. *Philosophical Transactions of the Royal Society, London A 306*, 147–159.

Holtedahl, H. 1984: High Pre-Late Weichselian sea-formed caves and other marine features on the Møre–Romsdal coast, West Norway. *Norsk Geologisk Tidsskrift 64*, 75–85.

Kaldhol, H. 1930: Sunnmøres kvartærgeologi. *Norsk Geologisk Tidsskrift 11*, 1–194.

Kellogg, T. B. 1977: Paleoclimatology and paleo-oceanography of the Norwegian and Greenland Seas: the last 450,000 years. *Marine Micropaleontology 2*, 234–249.

Kellogg, T. B., Duplessy, J. C. & Shackleton, N. J. 1978: Planktonic foraminiferal and oxygen isotopic stratigraphy and paleoclimatology of Norwegian Sea deep-sea cores. *Boreas 7*, 61–73.

Krinsley, D. H. & Doornkamp, J. 1973: *Atlas of Quartz Grain Surface Texture*. 91 pp. Cambridge University Press, Cambridge.

Landvik, J. Y. & Mangerud, J. 1985: A Pleistocene sandur in western Norway: facies relationships and sedimentological characteristics. *Boreas 14*, 161–174.

Larsen, E. & Holtedahl, H. 1985: The Norwegian strandflat: A reconsideration of its age and origin. *Norsk Geologisk Tidsskrift 65*, 247–254.

Larsen, E., Lie, R., Befring, S. & Longva, O. 1984: Weichsel stratigrafi i Skjonghelleren på Valderøya, Vest-Norge. *In* Larsen, E.: Weichsel stratigrafi og glasialgeologi på Nordvestlandet. Unpublished Dr. scient. thesis. University of Bergen.

Lauritzen, S.-E. 1984: Speleothem dating in Norway: an interglacial chronology. *Norsk Geografisk Tidsskrift 38*, p. 198.

Lauritzen, S.-E. & Gascoyne, M. 1980: The first radiometric dating of Norwegian stalagmites–evidence of pre-Weichselian karst caves. *Norsk Geografisk Tidsskrift 34*, 77–82.

Løvlie, R., Markussen, B., Sejrup, H. P. & Thiede, J. 1986: Magnetostratigraphy in three Arctic Ocean sediment cores: arguments for geomagnetic excurions within oxygen-isotope stage 2–3. *Physics of the Earth and Planetary Interiors 43*, 173–184.

Løvlie, R. & Sandnes, A. 1987: Palaeomagnetic excursions recorded in Mid-Weichselian cave sediments from Skjonghelleren, Valderøy, W-Norway. *Physics of the Earth and Planetary Interiors, 45*, 337–348.

Mangerud, J. 1981: The Early and Middle Weichselian in Norway: a review. *Boreas 10*, 381–393.

Mangerud, J. 1983: The glacial history of Norway. *In* Ehlers, J. (ed.): *Glacial Deposits in North-West Europe*, 3–9. A. A. Balkema, Rotterdam.

Mangerud, J., Andersen, S. Th., Berglund, B. E. & Donner, J. J. 1974: Quaternary stratigraphy of Norden, a proposal for terminology and classification. *Boreas 3*, 109–128.

Mangerud, J. & Berglund, B. E. 1978: The subdivision of the Quaternary of Norden: a discussion. *Boreas 7*, 179–181.

Mangerud, J., Gulliksen, S., Larsen, E., Longva, O., Miller, G. H. Sejrup, H.-P. & Sønstegaard, E. 1981a: A middle Weichselian ice-free period in Western Norway: The Ålesund Interstadial. *Boreas 10*, 447–462.

Mangerud, J., Larsen, E., Longva, O. & Sønstegaard, E. 1979: Glacial history of Western Norway 15,000–10,000 B.P. *Boreas 8*, 179–187.

Mangerud, J., Sønstegaard, E., Sejrup, H.-P. & Haldorsen, S. 1981b: A continuous Eemian–Early Weichselian sequence containing pollen and marine fossils at Fjøsanger, western Norway. *Boreas 10*, 137–208.

Miller, G. H., Sejrup, H. P., Mangerud, J. & Andersen, B. G. 1983: Amino acid ratios in Quaternary molluscs and foraminifera from western Norway: Correlation, geochronology and paleotemperature estimates. *Boreas 12*, 107–124.

Reite, A. J. 1967: Lokalglasiasjon på Sunnmøre. *Norges geologiske undersøkelse 247*, 262–287.

Reusch, H. 1877a: Nogle norske Huler. II Skjonghelleren. *Naturen 4*, 49–57.

Reusch, H. 1877b: Træk av Havets Virkninger på Norges Vestkyst. *Nyt Magazin for Naturvidenskaperne 22*, 169–244.

Reusch, H. 1913: En notis om vore havdannede huler. *Norsk Geologisk Tidsskrift 2*, 22–23.

Röthlisberger, H. 1972: Water pressure in intra and subglacial channels. *Journal of Glaciology 11*, 177–203.

Schrøder, I. 1984: Caves in non-limestone rocks of Norway. *Norsk Geografisk Tidsskrift 38*, 207–208.

Schwarcz, H. P. 1982: Applications of U-series dating to Archaeometry. *In* Ivanovich, M. & Harmon, R. S. (eds.): *Uranium Series Disequilibrium: Applications to Environmental Problems*, 302–325. Clarendon Press, Oxford.

Sejrup, H. P. 1987: Molluscan and foraminiferal biostratigraphy of an Eemian–Early Weichselian section on Karmøy, southwestern Norway. *Boreas 16*, 27–42.

Strass, I. F. 1978: Microtextures of quartz sand grains in coastal and shelf sediments, Møre, Western Norway. *Marine Geology 28*, 107–134.

Streeter, S. S., Belanger, P. E., Kellogg, T. G. & Duplessy, J. C. 1982: Late Pleistocene Paleo-Oceanography of the Norwegian–Greenland Sea: Benthic foraminiferal evidence. *Quaternary Research 18*, 72–90.

Symons, D. T. A., Stupavasky, M. & Gravenor, M. P. 1980: Remanence resetting by shock-induced thixotropy in the Seminary Till, Scarborough, Ontario, Canada. *Geological Society American Bulletin 91*, 593–598.

Szabo, B. J. 1980: Results and assessment of Uranium series dating of vertebrate fossils from Quaternary alluviums. *Arctic and Alpine Research 12*, 95–100.

Szabo, B. J. & Rosholt, J. N. 1982: Surficial continental sediments. *In* Ivanovich, M. & Harmon, R. S. (eds.): *Uranium Series Disequilibrium: Applications to Environmental Problems*, 246–267. Clarendon Press, Oxford.

Undås, I. 1942: On the Late-Quaternary history of Møre and Trøndelag (Norway). *Kongelige Norske Vitenskaps Selskaps Skrifter 2*. 92 pp.

Vibe-Müller, K. 1963: Arkeologiske undersøkelser av Skjonghelleren og området utenfor helleren kalt Hellersletta. Unpublished report, Historical Museum, University of Bergen.

Vorren, K.-D. 1978: Late and Middle Weichselian stratigraphy of Andøya, north Norway. *Boreas 7*, 19–38.

Whalley, W. B. & Krinsley, D. H. 1974: A scanning electron microscope study of surface textures of quartz grains from glacial environments. *Sedimentology 21*, 87–105.

White, W. B. 1976: Cave minerals and speleothems. *In* Ford, T. D. & Cullingford, C. H. H. (eds.): *The Science of Speleology*, 267–327. Academic Press, London.